

Manganese–Gold and –Silver Mixed-Metal Clusters Derived from the Unsaturated Binuclear Complex $[\text{Mn}_2(\text{CO})_6(\mu\text{-Ph}_2\text{PCH}_2\text{PPh}_2)]^{2-}$ ($\text{Mn}=\text{Mn}$) and Related Anions

Xiang-Yang Liu, Víctor Riera, and Miguel A. Ruiz*

Departamento de Química Orgánica e Inorgánica, I.U.Q.O.E.M., Universidad de Oviedo, E-33071 Oviedo, Spain

Maurizio Lanfranchi and Antonio Tiripicchio

Dipartimento di Chimica Generale ed Inorganica, Chimica Analitica, Chimica Fisica, Università di Parma, Parco Area delle Scienze 17/A, I-43100 Parma, Italy

Received June 16, 2003

Reaction of the unsaturated dihydride $[\text{Mn}_2(\mu\text{-H})_2(\text{CO})_6(\mu\text{-dppm})]$ with $\text{Li}[\text{BHET}_3]$ proceeds stepwise, giving first the anionic hydride $[\text{Mn}_2(\mu\text{-H})(\text{CO})_6(\mu\text{-dppm})]^-$ and then the dianion $[\text{Mn}_2(\text{CO})_6(\mu\text{-dppm})]^{2-}$, both having a formally double metal–metal bond. In contrast, reaction with $\text{Na}[\text{BH}_4]$ gives cleanly the fluxional anionic trihydride $[\text{Mn}_2(\mu\text{-H})\text{H}_2(\text{CO})_6(\mu\text{-dppm})]^-$, which is electron precise. A related electron-precise dianion, $[\text{Mn}_2(\text{CO})_8(\mu\text{-dppm})]^{2-}$, is readily prepared by reducing $[\text{Mn}_2(\text{CO})_8(\mu\text{-dppm})]$ with Na amalgam and is protonated by $[\text{NH}_4]\text{PF}_6$ to give the corresponding dihydride $[\text{Mn}_2\text{H}_2(\text{CO})_8(\mu\text{-dppm})]$. The unsaturated anions react cleanly with silver or gold complexes of the type $[\text{MCl}(\text{PR}_3)]$ ($\text{M} = \text{Ag}$, $\text{R} = \text{Cy}$; $\text{M} = \text{Au}$, $\text{R} = \text{Ph}$, $p\text{-tol}$) to give the corresponding trinuclear hydride clusters $[\text{Mn}_2\text{M}(\mu\text{-H})(\text{CO})_6(\mu\text{-dppm})(\text{PR}_3)]$ or the tetranuclear clusters $[\text{Mn}_2\text{M}_2(\text{CO})_6(\mu\text{-dppm})(\text{PR}_3)_2]$ (X-ray study for $\text{M} = \text{Au}$, $\text{R} = p\text{-tol}$). The trinuclear manganese–gold cluster adds CO easily to give the electron-precise $[\text{Mn}_2\text{Au}(\mu\text{-H})(\text{CO})_7(\mu\text{-dppm})\{\text{P}(p\text{-tol})_3\}]$, but the tetranuclear clusters react with simple donors in a more complex way. For example, reaction with $(\text{EtO})_2\text{POP}(\text{OEt})_2$ (tedip) gives a mixture of the corresponding tetranuclear derivatives $[\text{Mn}_2\text{Au}_2(\text{CO})_5(\mu\text{-dppm})(\text{PR}_3)(\mu\text{-tedip})]$, arising from substitution of peripheral CO and PR_3 ligands, and the trinuclear alkoxyphosphido clusters $[\text{Mn}_2\text{Au}\{\mu\text{-P}(\text{OEt})_2\}(\text{CO})_6(\mu\text{-dppm})(\text{PR}_3)]$, derived from the cleavage of a P–O bond in the backbone of the diphosphite ligand. The acid–base behavior of the tetranuclear digold clusters has been further explored through the reaction with $\text{HBF}_4\cdot\text{OEt}_2$, which gives the cationic hydride cluster $[\text{Mn}_2\text{Au}_2(\mu_3\text{-H})(\text{CO})_6(\mu\text{-dppm})\{\text{P}(p\text{-tol})_3\}_2]\text{BF}_4$, and the reaction with SnCl_2 , which gives the raft-type pentanuclear manganese–gold–tin cluster $[\text{Mn}_2\text{Au}_2\text{SnCl}_2(\text{CO})_6(\mu\text{-dppm})\{\text{P}(p\text{-tol})_3\}_2]$, characterized through an X-ray study.

Introduction

Some time ago we reported the reduction reaction of the dihydride $[\text{Mn}_2(\mu\text{-H})_2(\text{CO})_6(\mu\text{-dppm})]$ ($\text{dppm} = \text{Ph}_2\text{PCH}_2\text{PPh}_2$) to give alkali-metal salts of $[\text{Mn}_2(\text{CO})_6(\mu\text{-dppm})]^{2-}$ (**1**), an anionic complex displaying quite a nucleophilic behavior despite the formal unsaturation of the molecule.¹ Subsequent work established that the dppm bridge acts as a very efficient and robust ligand in this anion, preserving the dimetal substrate from disruption even under oxidation conditions.² Because of this, we decided to study in more detail the reactions of $[\text{Mn}_2(\mu\text{-H})_2(\text{CO})_6(\mu\text{-dppm})]$ with different reducing agents in order to get anionic derivatives closely related to **1**. As will be shown, we have thus been able to prepare the unsaturated hydride $[\text{Mn}_2(\mu\text{-H})(\text{CO})_6(\mu\text{-dppm})]^-$ (**2**)

and other related anions (Chart 1). Both **1** and **2** are 32-electron complexes; therefore, a double Mn–Mn bond can be formulated for these anions. The combination of multiple metal–metal bonds and negative charges is rare among the binuclear transition-metal carbonyl anions. In fact, there are only a few examples of those anions, such as the paramagnetic $[\text{Fe}_2(\mu\text{-P}^t\text{Bu}_2)_2(\text{CO})_5]^-$,³ the dihydrides $[\text{M}_2(\mu\text{-H})_2(\text{CO})_8]^{2-}$ ($\text{M} = \text{Cr}$, Mo , W),⁴ and the phosphide complexes $[\text{Fe}_2(\mu\text{-PPh}_2)(\text{CO})_6]^-$ ⁵ and $[\text{Mo}_2\text{Cp}_2(\mu\text{-PR}_2)(\mu\text{-CO})_2]^-$ ($\text{R} = \text{Cy}$, Ph , OEt ; $\text{Cp} = \text{C}_5\text{H}_5$).⁶ Therefore, exploring the chemistry of these unsaturated anions was a matter of added interest. In this paper we report the reactions of anions **1** and **2** toward gold and

* To whom correspondence should be addressed. E-mail: mara@saaron.quimica.uniovi.es.

(1) Liu, X. Y.; Riera, V.; Ruiz, M. A. *Organometallics* **1994**, *13*, 2925.

(2) Liu, X. Y.; Riera, V.; Ruiz, M. A.; Bois, C. *Organometallics* **2001**, *20*, 3007.

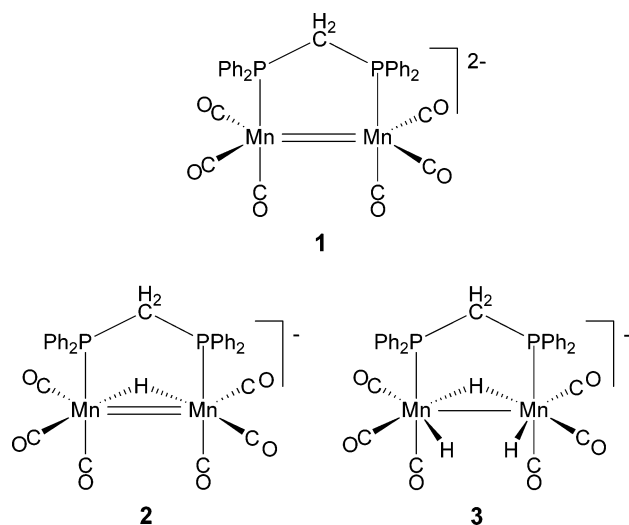
(3) Van der Linden, J. G. M.; Heck, J.; Walter, B.; Bottcher, H.-C. *Inorg. Chim. Acta* **1995**, *217*, 29.

(4) Lin, J. T.; Hagen, G. P.; Ellis, J. E. *J. Am. Chem. Soc.* **1983**, *105*, 2296 and references therein.

(5) Seyferth, D.; Brewer, K. S.; Wood, T. G.; Cowie, M.; Hiltz, R. W. *Organometallics* **1992**, *11*, 2570.

(6) García, M. E.; Melón, S.; Ramos, A.; Riera, V.; Ruiz, M. A.; Belletti, D.; Graiff, C.; Tiripicchio, A. *Organometallics* **2003**, *22*, 1983.

Chart 1



silver phosphine complexes of the type $[\text{MCl}(\text{PR}_3)]$. Although this is a classical synthetic route to heterometallic group 11–transition-metal compounds,⁷ the electron deficiency present in anions **1** and **2** makes these compounds rational synthetic precursors for unsaturated clusters having Mn–Au or Mn–Ag bonds, only a limited number of which are known,^{8–12} thus allowing the study of their chemical behavior. We have done this by investigating the reactions of the new unsaturated clusters with some simple acids and bases.

Results and Discussion

Anionic Hydrides Derived from $[\text{Mn}_2(\mu\text{-H})_2(\text{CO})_6(\mu\text{-dppm})]$. As we have reported previously, reactions of the title dihydride with Na amalgam, potassium, or an excess of $\text{Li}[\text{BHET}_3]$ gives the corresponding alkali-metal salt of anion **1**.² Under normal conditions, no intermediate species can be detected in these reactions. However, when using just 1 equiv of the lithium reagent, a dark brown solution is obtained, shown by IR and NMR to contain the unsaturated anion $[\text{Mn}_2(\mu\text{-H})(\text{CO})_6(\mu\text{-dppm})]^-$ (**2**, Li^+ salt) as the major species. We should stress that no other reagent was found to allow for a convenient synthesis of this intermediate anion.

Anion **2** is characterized by a single ^{31}P NMR resonance at 72.0 ppm (close to that for **1**) and CO stretching bands (Table 1) with a pattern similar to those of **1** or the parent dihydride, but having intermediate frequen-

cies as expected (average $\nu(\text{CO})$ values are 1833, 1894, and 1975 cm^{-1} for **1**, **2** and the parent dihydride, respectively). Moreover, anion **2** exhibits a triplet ^1H NMR resonance at -11.2 ppm, which is indicative of the presence of a bridging hydride symmetrically placed cis with respect to the diphosphine bridge ($J_{\text{PH}} = 28$ Hz, to be compared to $J_{\text{PH}} = 21$ Hz for the starting dihydride).¹³ All attempts to isolate this unstable anion resulted in its rapid decomposition.

As expected, anion **2** reacts with another 1 equiv of $\text{Li}[\text{BHET}_3]$ to yield **1**, and it also gives the starting dihydride upon reaction with $[\text{NH}_4]\text{PF}_6$. Surprisingly, protonation of **1** cannot be controlled so as to give **2**. Thus, when **1** is reacted with 1 equiv of $[\text{NH}_4]\text{PF}_6$, only the neutral dihydride and unreacted **1** are present in the reaction mixture.

Reaction of $[\text{Mn}_2(\mu\text{-H})_2(\text{CO})_6(\mu\text{-dppm})]$ with $\text{Na}[\text{BH}_4]$ also takes place easily in tetrahydrofuran solution but leads to a completely different result, as it gives cleanly the yellow-orange trihydride anion $[\text{Mn}_2(\mu\text{-H})_2(\text{CO})_6(\mu\text{-dppm})]^-$ (**3**, Na^+ salt, Chart 1). The IR spectrum for this electron-precise anion exhibits $\nu(\text{CO})$ bands in a region similar to those of **2**, and its ^{31}P NMR spectrum is also indicative of the chemical equivalence of both metal centers. However, the ^1H NMR spectrum of **3** exhibits a single and broad resonance at -13.98 ppm, with a relative intensity corresponding to 3 H atoms. All the above data are analogous to those found for $\text{Na}[\text{Mn}_2(\mu\text{-H})_2(\text{CO})_6(\mu\text{-tedip})]$ (tedip = $(\text{EtO})_2\text{POP}(\text{OEt})_2$), a fluxional trihydride anion prepared analogously from $[\text{Mn}_2(\mu\text{-H})_2(\text{CO})_6(\mu\text{-tedip})]$ and $\text{Na}[\text{BH}_4]$.¹⁰ We thus assume that anion **3** also experiences dynamic exchange between bridging and terminal hydride positions. Although we have not explored the reactivity of this anion in detail, initial experiments suggest that it behaves as the aforementioned tedip-bridged trihydride. For example, reaction of **3** with $[\text{CuCl}(\text{PPh}_3)]_4$ gives a trihydride Mn_2Cu cluster similar to $[\text{Mn}_2\text{Cu}(\mu\text{-H})_3(\text{CO})_6(\mu\text{-tedip})(\text{PPh}_3)]$.¹⁰

Preparation and Structural Characterization of $[\text{Mn}_2(\text{CO})_8(\mu\text{-dppm})]^{2-}$ (4**).** Although formally unsaturated, anions **1** and **2** do not react with CO to give an electron-precise anion. With the aim of finding a synthetic connection between electron-precise precursors and unsaturated anions, we attempted the synthesis of $[\text{Mn}_2(\text{CO})_8(\mu\text{-dppm})]^{2-}$ using conventional synthetic routes. This was easily accomplished by reacting the singly bonded $[\text{Mn}_2(\text{CO})_8(\mu\text{-dppm})]$ with Na amalgam in tetrahydrofuran, thus paralleling the metal–metal bond cleavage of unbridged $[\text{Mn}_2(\text{CO})_{10}]$ and $[\text{Mn}_2(\text{CO})_8\text{L}_2]$ complexes (L = phosphine or phosphite ligand).^{14,15}

The IR spectrum of anion **4** (Na^+ salt) in tetrahydrofuran solution exhibits five partially split CO stretching bands, while its ^{31}P NMR spectrum exhibits a single NMR resonance. The high number of IR bands (a total of eight) for **4** is indicative of substantial Na^+ –anion

(7) Reviews: (a) Robert, D. A.; Geoffroy, G. L. In *Comprehensive Organometallic Chemistry*; Wilkinson, G., Stone, F. G. A., Abel, E. W., Eds.; Pergamon: Oxford, U.K., 1982; Vol. 6, Chapter 40. (b) Salter, I. D. *Adv. Organomet. Chem.* **1989**, 29, 249. (c) Mingos, D. M. P.; Watson, M. J. *Adv. Inorg. Chem.* **1992**, 39, 327. (d) Salter, I. D. In *Comprehensive Organometallic Chemistry*, 2nd ed.; Abel, E. W., Stone, F. G. A., Wilkinson, G., Eds.; Pergamon: Oxford, U.K., 1995; Vol. 10, Chapter 5.

(8) Liu, X. Y.; Riera, V.; Ruiz, M. A.; Tiripicchio, A.; Tiripicchio-Camellini, M. *Organometallics* **1996**, 15, 974.

(9) Carreño, R.; Riera, V.; Ruiz, M. A.; Tiripicchio, A.; Tiripicchio-Camellini, M. *Organometallics* **1994**, 13, 993.

(10) (a) Riera, V.; Ruiz, M. A.; Tiripicchio, A.; Tiripicchio-Camellini, M. *Organometallics* **1993**, 12, 2962. (b) Riera, V.; Ruiz, M. A.; Tiripicchio, A.; Tiripicchio-Camellini, M. *J. Chem. Soc., Chem. Commun.* **1985**, 1505.

(11) Carreño, R.; Riera, V.; Ruiz, M. A.; Bois, C.; Jeannin, Y. *Organometallics* **1992**, 11, 2923.

(12) Haupt, H. J.; Heinekamp, C.; Flörke, U.; Juptner, U. *Z. Anorg. Allg. Chem.* **1992**, 608, 100.

(13) (a) García-Alonso, F. J.; Riera, V.; Ruiz, M. A.; Tiripicchio, A.; Tiripicchio-Camellini, M. *Organometallics* **1992**, 11, 370. (b) García-Alonso, F. J.; García-Sanz, M.; Riera, V.; Ruiz, M. A.; Tiripicchio, A.; Tiripicchio-Camellini, M. *Angew. Chem., Int. Ed. Engl.* **1988**, 27, 1167.

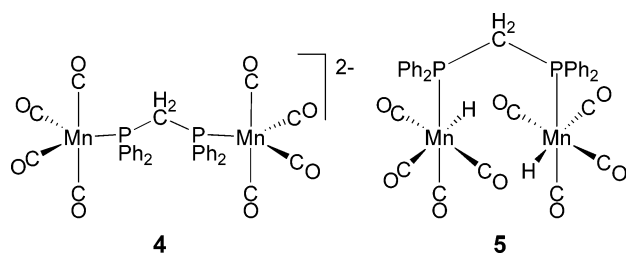
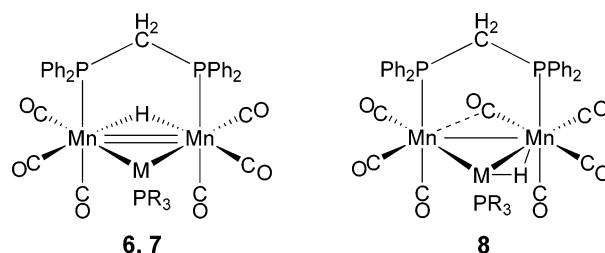
(14) (a) King, R. B. *Adv. Organomet. Chem.* **1964**, 2, 157. (b) Treichel, P. M. In *Comprehensive Organometallic Chemistry*; Wilkinson, G., Stone, F. G. A., Abel, E. W., Eds.; Pergamon: Oxford, U.K., 1982; Vol. 4, Chapter 29.

(15) Darensbourg, M. Y.; Darensbourg, D. J.; Burns, D.; Drew, D. A. *J. Am. Chem. Soc.* **1976**, 98, 3127.

Table 1. IR and $^{31}\text{P}\{^1\text{H}\}$ NMR Data for New Compounds

compd	$\nu_{\text{st}}(\text{CO})^a/\text{cm}^{-1}$	$\delta(\text{P})^b/\text{ppm}$
$\text{Na}_2[\text{Mn}_2(\text{CO})_6(\mu\text{-dppm})]$ (1)	1888 (s), 1841 (vs), 1817 (s), 1787 (s) ^c	67.0 ^d
$\text{Li}[\text{Mn}_2(\mu\text{-H})(\text{CO})_6(\mu\text{-dppm})]$ (2)	1967 (s), 1901 (vs), 1866 (s), 1840 (m) ^c	72.0 ^e
$\text{Na}[\text{Mn}_2(\mu\text{-H})\text{H}_2(\text{CO})_6(\mu\text{-dppm})]$ (3)	1983 (s), 1919 (vs), 1900 (m, sh), 1866 (m), 1843 (w) ^c	63.5
$\text{Na}_2[\text{Mn}_2(\text{CO})_8(\mu\text{-dppm})]$ (4)	1940 (s, sh), 1935 (s), 1850 (s), 1825 (s, sh), ^e 1816 (vs), 1803 (s, sh), 1755 (m, sh) ^c	88.9 ^d
$[\text{Mn}_2\text{H}_2(\text{CO})_8(\mu\text{-dppm})]$ (5)	2060 (m), 1992 (m), 1988 (m), 1966 (vs), 1947 (m, sh), 1928 (w) ^f	59.6 ^g
$[\text{Mn}_2\text{Ag}(\mu\text{-H})(\text{CO})_6(\mu\text{-dppm})(\text{PCy}_3)]$ (6)	1994 (vs), 1951 (vs), 1912 (m), 1881 (s)	66.5 (d, br), 30.8 (2 \times dt) ^h
$[\text{Mn}_2\text{Au}(\mu\text{-H})(\text{CO})_6(\mu\text{-dppm})\{\text{P}(p\text{-tol})_3\}]$ (7)	2002 (vs), 1966 (vs), 1922 (m), 1893 (s)	70.0 (t), ⁱ 65.2 (s, br) ^g
$[\text{Mn}_2\text{Au}(\mu\text{-H})(\text{CO})_7(\mu\text{-dppm})\{\text{P}(p\text{-tol})_3\}]$ (8)	2021 (s), 1950 (vs), 1931 (s), 1909 (m, sh), 1869 (m)	64.0 (s, br), 46.4 (s)
$[\text{Mn}_2\text{Ag}_2(\text{CO})_6(\mu\text{-dppm})(\text{PCy}_3)_2]$ (9)	1954 (m), 1910 (vs), 1876 (w), 1850 (s)	73.1 (tt), 29.2 (2 \times dt) ^j
$[\text{Mn}_2\text{Au}_2(\text{CO})_6(\mu\text{-dppm})(\text{PPh}_3)_2]$ (10a)	1972 (s), 1935 (vs), 1896 (w), 1870 (s)	66.9 (br), 64.9 (t) ^k
$[\text{Mn}_2\text{Au}_2(\text{CO})_6(\mu\text{-dppm})\{\text{P}(p\text{-tol})_3\}_2]$ (10b)	1972 (s), 1936 (vs), 1899 (w), 1871 (s)	69.2 (br), 65.7 (t) ^k
$[\text{Mn}_2\text{Au}_2(\text{CO})_5(\mu\text{-dppm})(\text{PPh}_3)(\mu\text{-tedip})]$ (11a)	1981 (m), 1928 (vs), 1912 (m, sh), 1893 (m), 1851 (w)	Table 3
$[\text{Mn}_2\text{Au}_2(\text{CO})_5(\mu\text{-dppm})\{\text{P}(p\text{-tol})_3\}(\mu\text{-tedip})]$ (11b)	1980 (m), 1928 (vs), 1910 (m, sh), 1893 (m), 1852 (w)	Table 3
$[\text{Mn}_2\text{Au}\{\mu\text{-P}(\text{OEt})_2\}(\text{CO})_6(\mu\text{-dppm})(\text{PPh}_3)]$ (12a)	1994 (s), 1962 (vs), 1919 (m), 1902 (sh, s), 1894 (s)	Table 3
$[\text{Mn}_2\text{Au}\{\mu\text{-P}(\text{OEt})_2\}(\text{CO})_6(\mu\text{-dppm})\{\text{P}(p\text{-tol})_3\}_2]$ (12b)	1993 (s), 1962 (vs), 1919 (m), 1902 (sh, s), 1893 (s)	Table 3
$[\text{Mn}_2\text{Au}_2(\mu\text{-H})(\text{CO})_6(\mu\text{-dppm})\{\text{P}(p\text{-tol})_3\}_2]\text{BF}_4$ (13)	2015 (s), 1986 (vs), 1949 (m), 1924 (s)	63.7 (br), 62.7 (s, br)
$[\text{Mn}_2\text{Au}_2\text{SnCl}_2(\text{CO})_6(\mu\text{-dppm})\{\text{P}(p\text{-tol})_3\}_2]$ (14)	1991 (vs), 1943 (s), 1927 (s), 1890 (m), 1860 (m)	51.5 (false t), 49.9 (s, br) ^l

^a In dichloromethane solution, unless otherwise stated. ^b Measured at 121.5 MHz, in CD_2Cl_2 solution at room temperature, unless otherwise stated; coupling constants (J) in Hz. ^c In tetrahydrofuran (THF) solution. ^d In $\text{THF}/\text{C}_6\text{D}_6$ (9/1) solution. ^e In $\text{THF}/\text{D}_2\text{O}$ solution. ^f In petroleum ether solution. ^g In C_6D_6 solution. ^h Recorded at 233 K, $J(\text{Ag}-\text{PPh}) = 12$, $J(^{109}\text{Ag}-\text{PCy}) = 358$, $J(^{107}\text{Ag}-\text{PCy}) = 310$, $J(\text{PP}) = 7$. ⁱ $\text{Au}-\text{P}$; $J(\text{PP}) = 14$. ^j Recorded at 218 K; $J(\text{Ag}-\text{PPh}) = 16$, $J(^{109}\text{Ag}-\text{PCy}) = 358$, $J(^{107}\text{Ag}-\text{PCy}) = 311$, $J(\text{PP}) = 6$. ^k $J(\text{PP}) = 14$. ^l $|J(\text{PP}) + J(\text{PP}')| = 16$; when recorded at 188 K δ 52.4 (s, br, $J(\text{PSn}) = 243$), 46.9 (s, br, $J(\text{PSn}) = 175$).

Chart 2**Chart 3**

interactions, this being common in mononuclear carbonylates.¹⁶ In fact, the IR spectrum of **4** is very similar to that reported for $\text{Na}[\text{Mn}(\text{CO})_4(\text{PMe}_2\text{Ph})]$ in tetrahydrofuran (1940.8 (m)*, 1934.7 (w), 1847.6 (m), 1817.1 (s), 1802.5 (m), 1767 (m)* cm^{-1} , with the asterisks labeling the bands attributed to the Na^+ -anion pairs).¹⁵ In the latter anion, the phosphine ligand occupies an axial position (C_{3v} symmetry). However, the high-frequency bands for **4** are of high intensity, which is indicative of a lower symmetry. Therefore, we propose that the P atoms in **4** occupy equatorial positions (local C_{2v} symmetry), which perhaps could be explained on steric grounds.

As expected, anion **4** is easily protonated to give the corresponding dihydride $[\text{Mn}_2\text{H}_2(\text{CO})_8(\mu\text{-dppm})]$ (**5**) in high yield. The IR spectrum for **5** in the CO stretching region is very similar to those for the halide complexes $[\text{Mn}_2\text{X}_2(\text{CO})_8(\mu\text{-tedip})]$,¹⁷ and thus a similar structure is assumed for **5**, with two *cis*- $\text{Mn}(\text{CO})_4\text{H}$ fragments joined by the dppm bridge (Chart 2). In agreement with this proposal, the ^1H NMR spectrum of **5** displays a relatively poorly shielded resonance (δ -7.26 ppm), indicative of terminal coordination, and an H-P coupling around 40 Hz (for comparison, the hydride ligand in *fac*- $[\text{MnH}(\text{CO})_3(\text{Ph}_2\text{PCH}_2\text{CH}_2\text{PPh}_2)]$ gives rise to a triplet resonance at δ -7.8 ppm with $J_{\text{PH}} = 45$ Hz).¹⁸

Compound **5** might be considered as a convenient precursor for the unsaturated $[\text{Mn}_2(\mu\text{-H})_2(\text{CO})_6(\mu\text{-dppm})]$,

the latter currently requiring the completion of some tedious synthetic steps.¹³ Unfortunately, those expectations have not been fulfilled. Although we have found that irradiation with UV-visible light of toluene or tetrahydrofuran solutions of **5** at -40°C gives indeed some of the targeted dihydride, this reaction has a poor selectivity and also gives considerable amounts of the known complexes $[\text{Mn}_2(\mu\text{-}\eta^1\text{:}\eta^2\text{-CO})(\text{CO})_4(\mu\text{-dppm})_2]$ ¹⁹ and $[\text{Mn}_2(\mu\text{-H})_2(\text{CO})_4(\mu\text{-dppm})_2]$;²⁰ therefore, the reaction has no synthetic utility. Noticeably, the reverse reaction does not occur either. In fact, carbonylation of the unsaturated $[\text{Mn}_2(\mu\text{-H})_2(\text{CO})_6(\mu\text{-dppm})]$ gives the metal-metal bonded $[\text{Mn}_2(\text{CO})_8(\mu\text{-dppm})]$ rather than dihydride **5**.

Silver and Gold Derivatives of Hydride Anion

2. The Li^+ salt of anion **2**, prepared in situ as described above, reacts rapidly with equivalent amounts of the halide complexes $[\text{AgCl}(\text{PCy}_3)]_4$ and $[\text{AuCl}\{\text{P}(p\text{-tol})_3\}]$ to give the corresponding mixed-metal hydride clusters $[\text{Mn}_2\text{M}(\mu\text{-H})(\text{CO})_6(\mu\text{-dppm})(\text{PR}_3)]$ (**6**, $\text{M} = \text{Ag}$, $\text{R} = \text{Cy}$; **7**, $\text{M} = \text{Au}$, $\text{R} = p\text{-tol}$) (Chart 3). As concluded from the analysis of the corresponding spectroscopic data (Table 1 and Experimental Section), these blue-violet compounds are completely analogous to the Au-Mn clusters $[\text{Mn}_2\text{Au}(\mu\text{-H})(\text{CO})_6(\mu\text{-L}_2)(\text{PPh}_3)]$, prepared from the corresponding dihydride $[\text{Mn}_2(\mu\text{-H})_2(\text{CO})_6(\mu\text{-L}_2)]$ and $[\text{AuMe}(\text{PPh}_3)]$ ($\text{L}_2 = \text{tedip}$,¹⁰ dppm¹¹). We recall here that the

(16) Darensbourg, M. Y. *Prog. Inorg. Chem.* **1985**, 33, 221.

(17) Riera, V.; Ruiz, M. A. *J. Chem. Soc., Dalton Trans.* **1986**, 2617.

(18) Booth, B. L.; Haszeldine, R. N. *J. Chem. Soc. A* **1966**, 157.

(19) Colton, R.; Commons, C. J. *Aust. J. Chem.* **1975**, 28, 1673.

(20) Aspinall, H. C.; Deeming, A. J. *J. Chem. Soc., Chem. Commun.* **1983**, 838.

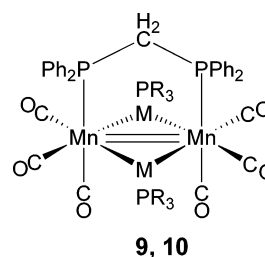
tedip-bridged compound exhibits a very short value of 2.739(3) Å for the Mn–Mn distance, in agreement with the electronic unsaturation of all these clusters, which retain a formally double Mn–Mn bond. From a synthetic point of view, anion **2** thus represents an alternative preparative route to Mn–Au compounds but is still a unique entry to unsaturated Mn–Ag clusters. As we will see below, the same applies to anion **1**.

The presence of the hydride ligand in complexes **6** and **7** is clearly denoted by the appearance of a quite shielded resonance at ca. –21 ppm in their ^1H NMR spectra. In addition, the silver nuclei in **6** exhibit a small two-bond coupling to the bridging diphosphine (12 Hz) and large one-bond coupling to the PCy_3 phosphorus atom, as expected. The absence of two-bond H–Ag coupling in **6** is somewhat unexpected, as values of 12–24 Hz have been measured for the electron-precise clusters $[\text{Mn}_4\text{Ag}_2(\mu\text{-H})_6(\text{CO})_{12}(\mu\text{-tedip})_2]^9$ and $[\text{Mn}_2\text{Ag}(\mu\text{-H})_3(\text{CO})_6(\mu\text{-tedip})(\text{PPh}_3)]^{10}$. This difference might be related to the unsaturated nature of **6**, expected to display a Mn–Mn separation ca. 0.5 Å shorter than the saturated clusters, whereby substantial changes in the H–Mn–Ag angles are to be expected. It is well-known that two-bond coupling is quite sensitive to the bond angle involved and that the coupling constant might even change from negative to positive values upon an increase in the bond angle.²¹

Compounds **6** and **7** are electron deficient and therefore expected to add simple ligands easily. Indeed, the Mn–Au cluster adds carbon monoxide easily, to give the electron-precise $[\text{Mn}_2\text{Au}(\mu\text{-H})(\text{CO})_7(\mu\text{-dppm})\{\text{P}(p\text{-tol})_3\}]$ (**8**). Spectroscopic data for this complex (Table 1 and Experimental Section) indicate that the uptake of a CO ligand causes a dramatic structural rearrangement in the molecule, whereby the hydride ligand moves from a $\text{Mn}_2(\mu\text{-H})$ position into a $\text{Mn}(\mu\text{-H})\text{Au}$ one, as deduced from its considerably low shielding (δ –5.43 ppm) and large coupling to the P atom on gold ($J_{\text{HP}} = 92$ Hz), well inside the range found for H atoms bridging M–AuPR₃ bonds (80–110 Hz).^{22,23} The presence of a single resonance in the ^{31}P NMR spectrum and the grouping of the carbonyl ^{13}C resonances into a 1:2:4 pattern might suggest the presence of a plane of symmetry relating both manganese moieties in **8**. This would imply the presence of a bridging carbonyl. However, the latter is inconsistent with the absence of the characteristic spectroscopic features for this coordination mode of CO (high ^{13}C chemical shift and low CO stretching frequency). The situation is thus analogous to that encountered for the related tedip-bridged cluster $[\text{Mn}_2\text{Au}(\mu\text{-H})(\text{CO})_7(\mu\text{-tedip})(\text{PPh}_3)]$, which was found to have an asymmetric fluxional structure.¹⁰ We then propose for **8** a similar structure (Chart 3), although we have found no direct experimental evidence for this fluxional behavior. In fact, the P atoms of the diphosphine ligand in **8** remained equivalent in the ^{31}P spectrum down to 188 K.

Silver and Gold Derivatives of Anion 1. The Na^+ salt of anion **1** reacts rapidly in tetrahydrofuran with 2

Chart 4



equiv of $[\text{AgCl}(\text{PCy}_3)]_4$ or $[\text{AuCl}(\text{PR}_3)]$ to give the corresponding tetranuclear clusters $[\text{Mn}_2\text{M}_2(\text{CO})_6(\mu\text{-dppm})(\text{PR}_3)_2]$ (**9**, M = Ag, R = Cy; **10a**, M = Au, R = Ph; **10b**, M = Au, R = *p*-tol) in good yields (Chart 4). No intermediate trinuclear clusters were detected when using just 1 equiv of the silver or gold complexes, thus paralleling our inability to stop the protonation reaction so as to yield anion **2** from **1**.

The structure of **10b** has been determined through an X-ray study and is depicted in Figure 1, while Table 2 collects some relevant bond lengths and angles. The cluster can be viewed as two $\text{Mn}(\text{CO})_3$ moieties bridged by the diphosphine and by two $\text{Au-P}(p\text{-tol})_3$ fragments; thus, a distorted-octahedral environment around each Mn atom can be envisaged. The Mn_2Au_2 core is in a flattened-butterfly arrangement, with the two AuMn_2 wings forming a dihedral angle of $17.51(9)^\circ$. The octahedral geometry for the Mn atoms and the digonal geometry for the Au atoms can be better explained by considering three-center–two-electron (3c–2e) bonds involving orbitals pointing toward the centers of the two Mn_2Au triangles. The short Mn–Mn separation of 2.865(4) Å is in agreement with the two 3c–2e bonds and is also consistent with the formal double Mn–Mn bond expected for this molecule on the basis of the EAN rule. Indeed, this value is significantly shorter than those found in the related electron-precise cluster $[\text{Mn}_2\text{Au}(\mu\text{-Br})(\text{CO})_6(\mu\text{-tedip})(\text{PR}_3)]$ (3.090(2) Å),²⁴ while it is identical within experimental error to that found in $[\text{Mn}_2\text{Au}_2(\mu_3\text{-H})(\text{CO})_6(\mu\text{-dppm})(\text{PR}_3)]\text{PF}_6$ (2.864(5) Å),¹¹ a cationic cluster isoelectronic with clusters **9** and **10** (see below). However, these figures are significantly higher than those measured in the isolobal-related compounds $[\text{Mn}_2(\mu\text{-H})_2(\text{CO})_6(\mu\text{-dppm})]$ (2.699(2) Å)^{13b} and $[\text{Mn}_2\text{Au}(\mu\text{-H})(\text{CO})_6(\mu\text{-tedip})(\text{PR}_3)]$ (2.739(3) Å).¹⁰ We interpret this as a steric effect derived from the close proximity of the relatively bulky dppm and $\text{P}(p\text{-tol})_3$ ligands, and this effect also would give a rationale for the significant bending of one of the $\text{Au-P}(p\text{-tol})_3$ groups away from the dppm bridge. As can be appreciated through the projection of the molecule along the Mn–Mn bond, the Au(1)–P(3) atoms lie in a plane almost perpendicular to the average Mn(1)Mn(2)P(1)P(2) plane, as expected. In contrast, the Au(2)–P(4) atoms are significantly displaced away from that plane. This can be attributed to the close proximity between one of the phenyl groups bonded to P(1) and a *p*-tolyl ring on P(4), these having C–H...C separations in the range 3.1–3.2 Å, which are close to the sum of the van der Waals radii for H and C atoms (ca. 3.0 Å). This means that the Au(2)P(*p*-tol)₃ bridging group cannot get any closer

(21) Jameson, C. J. In *Phosphorus-31 NMR Spectroscopy in Stereochemical Analysis*; Verkade, J. G., Quin, L. D., Eds.; VCH: Deerfield Beach, FL, 1987; Chapter 6.

(22) Green, M.; Orpen, A. G.; Salter, I. D.; Stone, F. G. A. *J. Chem. Soc., Dalton Trans.* **1984**, 2497.

(23) Albinati, A.; Auklin, C.; Janser, P.; Lehner, H.; Matt, D.; Pregosin, P. S.; Venzani, L. M. *Inorg. Chem.* **1989**, 28, 1105.

(24) Riera, V.; Ruiz, M. A.; Tiripicchio, A.; Tiripicchio-Camellini, M. *J. Chem. Soc., Dalton Trans.* **1987**, 1551.

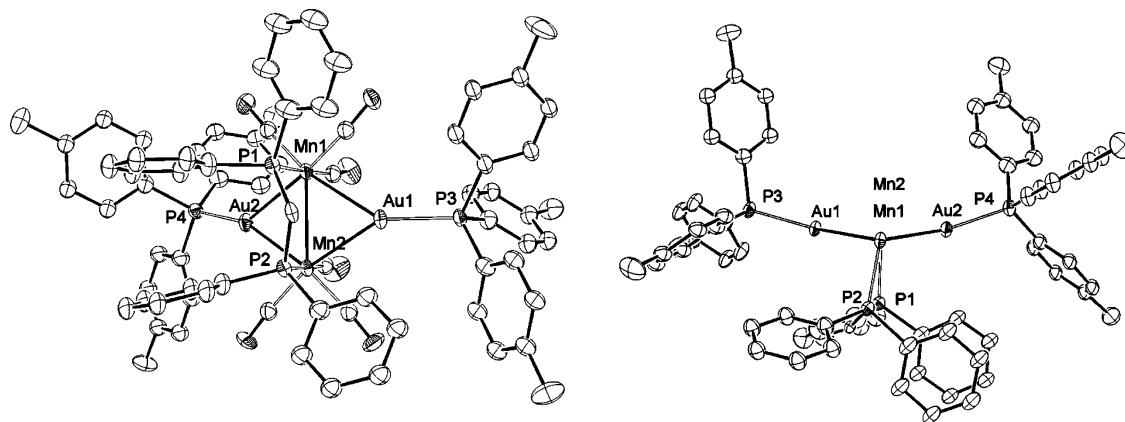


Figure 1. Molecular structure of compound **10b** (left) and its projection along the Mn–Mn bond (right; CO ligands omitted for clarity). Ellipsoids represent 30% probability.

Table 2. Selected Bond Lengths (Å) and Angles (deg) for Compounds **10b and **14****

Compound 10b			
Mn(1)–Mn(2)	2.865(4)	Mn(2)–Au(1)	2.672(3)
Mn(1)–Au(1)	2.696(3)	Mn(2)–Au(2)	2.669(3)
Mn(1)–Au(2)	2.690(3)	P(2)–Mn(2)	2.320(5)
P(1)–Mn(1)	2.308(5)	P(4)–Au(2)	2.342(4)
P(3)–Au(1)	2.339(4)		
Au(2)–Mn(1)–Au(1)	112.60(10)	Au(2)–Mn(2)–Au(1)	114.09(10)
Mn(2)–Au(1)–Mn(1)	64.51(8)	Mn(2)–Au(2)–Mn(1)	64.64(8)
P(1)–Mn(1)–Au(2)	99.63(14)	P(2)–Mn(2)–Au(2)	106.03(14)
P(1)–Mn(1)–Au(1)	96.72(14)	P(2)–Mn(2)–Au(1)	89.10(13)
P(1)–Mn(1)–Mn(2)	91.51(15)	P(2)–Mn(2)–Mn(1)	90.34(15)
Compound 14			
Mn(1)–Mn(2)	3.171(9)	Au(2)–Mn(2)	2.654(6)
Au(1)–Mn(1)	2.651(7)	Sn–Mn(2)	2.600(7)
Sn–Mn(1)	2.602(7)	Au(2)–Sn	2.815(4)
Au(1)–Sn	2.813(4)	Au(2)–P(4)	2.296(11)
Au(1)–P(3)	2.303(11)	Au(2)–C(4)	2.53(4)
Au(1)–C(1)	2.63(6)	Sn–Cl(2)	2.428(11)
Sn–Cl(1)	2.401(10)	Mn(2)–P(2)	2.335(13)
Mn(1)–P(1)	2.345(14)		
Sn–Mn(1)–Mn(2)	52.43(17)	Sn–Mn(2)–Mn(1)	52.47(17)
Sn–Mn(1)–Au(1)	64.75(16)	Sn–Mn(2)–Au(2)	64.79(16)
Au(1)–Mn(1)–Mn(2)	116.9(2)	Au(2)–Mn(2)–Mn(1)	117.2(2)
P(1)–Mn(1)–Mn(2)	88.1(4)	P(2)–Mn(2)–Mn(1)	91.0(4)
Mn(1)–Au(1)–Sn	56.77(15)	Mn(2)–Au(2)–Sn	56.68(14)
Cl(1)–Sn–Cl(2)	98.7(4)	Mn(2)–Sn–Mn(1)	75.1(2)
Mn(1)–Sn–Au(1)	58.47(15)	Mn(2)–Sn–Au(2)	58.53(15)
Au(1)–Sn–Au(2)	167.82(13)		

to the dpmm bridge without experiencing severe repulsion with the phenyl rings. An indirect evidence for the steric origin of the lengthening of the Mn–Mn vector in **10b** comes from comparison with the closely related series of clusters of formula $[\text{Os}_3(\mu\text{-X})_2(\text{CO})_{10}]$ ($\text{X} = \text{H}$, AuPPh_3), where the double Os–Os bonds display values almost independent of X, these being 2.681(1),^{25a} 2.699(1),^{25b} and 2.684(1) Å,^{25c} for the Os_3 , Os_3Au , and Os_3Au_2 clusters, respectively.

Spectroscopic data for **10b** in solution (Table 1 and Experimental Section) are consistent with its solid-state structure. Its IR spectrum exhibits four strong CO stretching bands, in agreement with a C_{2v} symmetry, with frequencies some 30 cm^{-1} lower than those for **7**, as expected when a bridging H is replaced by the less

electronegative AuPPh_3 fragment.¹⁰ Moreover, spectroscopic data are similar for **9** and **10a,b**, therefore indicating that all these tetranuclear clusters have the same structure. For the silver cluster **9** the average CO stretching frequency is some 22 cm^{-1} lower than that value for the gold clusters **10**, almost doubling the difference calculated between **6** and **7**, thus revealing the presence of additive effects. Other spectroscopic features for the Ag-PCy_3 fragments are very similar to those found in **6**, thus indicating a very similar binding of the $\mu\text{-AgPCy}_3$ groups.

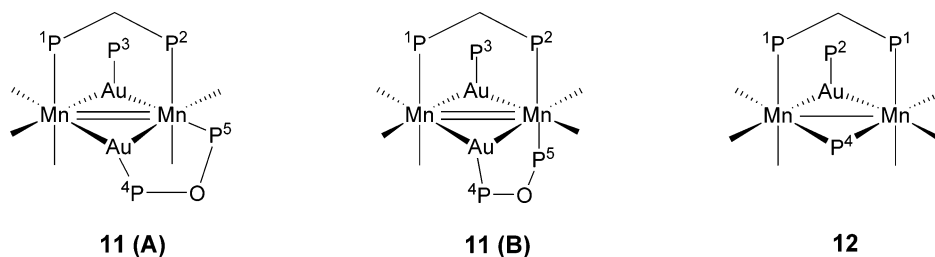
The presence of the basic PCy_3 phosphine gives substantial stability to the disilver cluster **9**. In fact, a similar Mn_2Ag_2 cluster can be prepared by reacting **1** and $[\text{AgCl}\{\text{P}(p\text{-tol})_3\}]_4$, but this product experiences progressive decomposition during all attempts at purification (crystallization, chromatography, etc.). We trust that this is a genuine electronic effect, so that AgPR_3 fragments would become overly strong oxidants when they have electron-withdrawing R groups. In agreement with this, all attempted reactions between **1** and $[\text{CuCl}(\text{PR}_3)]_4$ complexes lead to electron transfer rather than formation of heterometallic Mn_2Cu_2 clusters.

The synthetic value of anion **1** can be grasped from the fact that the tetranuclear clusters **9** and **10** are among the first examples of unsaturated Mn_2M_2 clusters to be reported. We have previously described a moderate-yield synthesis for a closely related Mn_2Au_2 cluster, prepared through the photochemical reaction between $[\text{Mn}_2\text{Au}(\mu\text{-H})(\text{CO})_6(\mu\text{-tedip})(\text{PR}_3)]$ and $[\text{AuMe}(\text{PPh}_3)]$. However, this synthetic method does not work with the dpmm-bridged compounds nor can it be obviously used in the preparation of silver derivatives.

Acid–Base Chemistry of the Unsaturated Clusters **10.** Compounds **10** are related to dihydrides $[\text{Mn}_2(\mu\text{-H})_2(\text{CO})_6(\mu\text{-L}_2)]$ through the isolobal analogy H/AuPPh_3 .²⁶ Thus, a similar chemical behavior between all these species is to be expected. However, the lower electronegativity of the gold fragment relative to hydrogen, clearly denoted by the values of the CO stretching frequencies already mentioned, expectedly should make compounds **10** to be better donors and poorer acceptors than the parent dihydrides. Besides, we have recognized the presence of some steric pressure in the

(25) (a) Churchill, M. R.; Hollander, F. J.; Hutchinson, P. *Inorg. Chem.* **1977**, *16*, 2697. (b) Burgess, K.; Johnson, B. F. G.; Kaner, D. A.; Lewis, J.; Raithby, P. R.; Azman, S. N.; Syed-Mustaffa, B. *J. Chem. Soc., Chem. Commun.* **1983**, 455. (c) Johnson, B. F. G.; Kaner, D. A.; Lewis, J.; Raithby, P. R. *J. Organomet. Chem.* **1981**, *215*, C33.

(26) Evans, D. G.; Mingos, D. M. P. *J. Organomet. Chem.* **1982**, *232*, 171.

Table 3. $^{31}\text{P}\{^1\text{H}\}$ NMR Data for Compounds **11** and **12**^a

compd	δ/ppm					$J(\text{PP})/\text{Hz}$					
	P(1)	P(2)	P(3)	P(4)	P(5)	12	14	24	25	35	45
11a (isomer A) ^b	68.3 (dd)	48.6 (d)	53.4 (s)	181.5 (m)	186.3 (br, d)	145	50				65
11b (isomer A) ^c	70.3 (dd)	48.3 (d)	52.7 (s)	182.4 (dd)	187.6 (d)	150	51				65
11a (isomer B) ^b	70.1 (dd)	60.3 (ddd)	57.4 (d)	184.4 (m)	179.8 (m)	152	58	15	52	20	60
11b (isomer B) ^c	71.8 (dd)	59.6 (ddd)	56.5 (d)	185.7 (br, td)	181.9 (br, td)	152	58	14	53	22	60
12a ^d	56.3 (dd)	65.9 (t)		420.6 (t)			11	33			
12b	56.4 (dd)	64.7 (t)		420.8 (t)			11	33			

^a Measured at 162.0 MHz, in CD_2Cl_2 solution at room temperature, unless otherwise stated; coupling constants (J) in Hz. Labeling is given according to the figure below. ^b **A**:**B** = 1:2. ^c In C_6D_6 solution. ^d Recorded at 243 K.

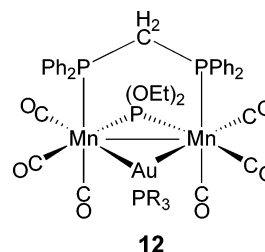
structure of **10b**, a fact that could also have a significant effect on the reactivity of these clusters.

We have checked the general acid–base behavior of these tetranuclear clusters by studying some reactions of **10** with simple donors (CO, phosphines), with pure acceptors (H^+), and with some fragments related to the methylene fragment, which then involve both donor and acceptor interactions with the metal substrate.

In contrast with the behavior observed for the trinuclear cluster **7**, the digold clusters **10** do not react with CO under ordinary conditions of temperature and pressure. We view this as an effect of the increased electron density at the dimanganese center when replacing H by AuPR_3 moieties, thus reducing the overall acidity. As expected, reaction occurs when using stronger donors as phosphines, although results are strongly dependent on the added ligand. For example, PMe_3 reacts instantaneously with compounds **10** by completely destroying the clusters, thus giving products of the type $[\text{Mn}_2(\text{CO})_4(\mu\text{-dppm})(\text{PMe}_3)_2(\text{PR}_3)_2]$, which were not fully characterized. In contrast, the less basic and bidentate ligands dppm and tedip react rapidly with **10** without breakdown of the metal core.

We have studied in detail the reactions of clusters **10** with tedip. These take place within a few minutes at 0 °C to give in both cases a black-blue intermediate which could not be fully characterized. The latter intermediates rearrange at room temperature to give the corresponding blue-violet pentacarbonyl clusters $[\text{Mn}_2\text{Au}_2(\text{CO})_5(\mu\text{-dppm})(\text{PR}_3)(\mu\text{-tedip})]$ (**11a,b**) and the orange, electron-precise clusters $[\text{Mn}_2\text{Au}\{\mu\text{-P}(\text{OEt})_2\}(\text{CO})_6(\mu\text{-dppm})(\text{PR}_3)]$ (**12a,b**). Clusters **11** and **12** were obtained in all cases in a ca. 3:1 ratio. This product distribution was found to be rather insensitive to experimental conditions such as reaction time and solvent.

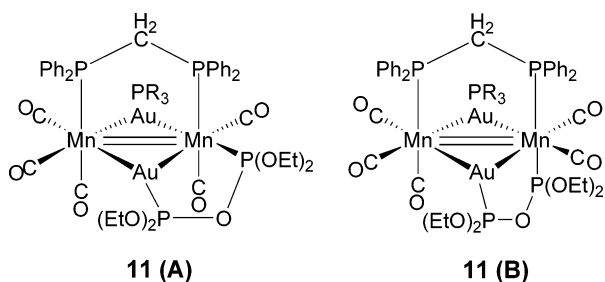
Spectroscopic data for **12** (Tables 1 and 3 and Experimental Section) allow for a complete characterization of these clusters. The presence of an unexpected diethoxyphosphide group is readily apparent from the ^{31}P NMR spectra, which exhibit in both cases a strongly deshielded resonance at ca. 420 ppm, a value very close to those measured for all clusters derived from the anion $[\text{Mn}_2\{\mu\text{-P}(\text{OEt})_2\}\{\mu\text{-OP}(\text{OEt})_2\}(\text{CO})_6]^{2-}$.⁸ The ^{31}P and ^1H

Chart 5

NMR spectra also confirm that a dppm ligand bridges equivalent manganese centers and that just a gold-bonded phosphine remains in these complexes. Finally, the IR spectrum of complexes **12** exhibits the five-band pattern characteristic of hexacarbonyl $[\text{Mn}_2(\mu\text{-X})(\mu\text{-Y})(\text{CO})_6(\mu\text{-L}_2)]$ complexes having *fac*- $\text{Mn}(\text{CO})_3$ oscillators (X, Y = one- or three-electron-donor ligands). In fact, CO stretching frequencies are quite similar to those for **7** (Table 1). All these data unambiguously define for complexes **12** the structure depicted in Chart 5. This structure is completely analogous to that determined crystallographically for $[\text{Mn}_2\text{Au}(\mu\text{-Br})(\text{CO})_6(\mu\text{-tedip})(\text{PPh}_3)]$.²⁴

Structural characterization for the violet clusters **11** is less straightforward. Although we were not able to grow good-quality crystals of those compounds, the available spectroscopic data allow us to establish both the composition and the main structural features of these compounds (Tables 1 and 3 and Experimental Section). In the first place, the IR spectra of compounds **11** differ from those recorded for the hexacarbonyl compounds described above. The absence of one of the two characteristic high-frequency CO bands suggests the presence of a pentacarbonyl $(\text{CO})_3\text{MnMn}(\text{CO})_2$ oscillator in the molecule. On the other hand, the ^{31}P and ^1H NMR spectra indicate that clusters **11** exist in solution as a mixture of two isomers in each case, labeled **A** and **B** (Chart 6 and Table 3). Each isomer contains one tedip bridge, one dppm bridge, and just one gold-bonded phosphine ligand. The ratio of isomers does not change significantly with temperature but is somewhat solvent-dependent. All the above data suggest that isomers **11** are just the result of replacing a

Chart 6



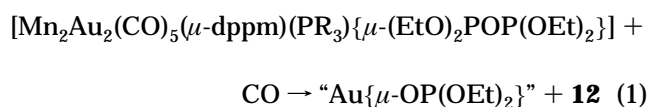
phosphine and a carbonyl group in clusters **10** by a tedip bridge. There are precedents of these substitution reactions in heterometallic carbonyl clusters containing group 11 element MPR₃ fragments.^{7d}

The assignment of ³¹P NMR resonances for clusters **11** (Table 3) is based on the assumption that the shift for P(1) should be very similar to those in clusters **10** and should not change much from one isomer to other, because of the similarity in the relevant chemical environments. From this, assignment of P(2) follows through its large PP coupling. This leads in turn to identify the gold-bonded P(3) as a weakly (isomer **B**) or not coupled (isomer **A**) resonance, as expected.

Isomers **A** and **B** strongly differ (by ca. 11 ppm) in the chemical shift of the diphosphine P(2) resonance, which we attribute to a change in the ligand trans to that phosphorus atom. We then assign the lowest shift to the isomer having P(2) trans to the better π -acceptor ligand (CO). The inequivalent phosphorus atoms of the tedip ligand in these isomers give rise to broad, ill-resolved multiplets at ca. 180 ppm. Despite this, the coupling constants between these P atoms and the dppm or phosphine ligands are consistent with the proposed structures.

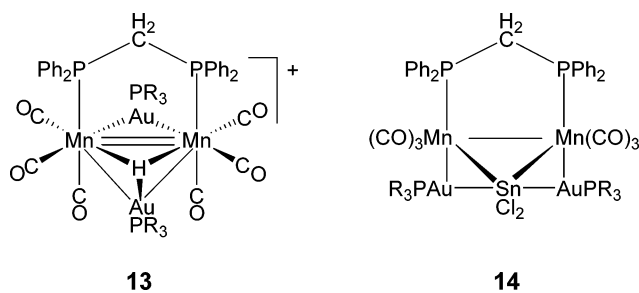
From a geometric point of view, the structure proposed for isomers **A** is strongly related to those recently determined for three electron-precise Mn–Au clusters of general formula [Mn₂Au(μ -PPh₂)(CO)₇(μ -L₂)],²⁷ in which a diphosphine ligand (L₂) bridges one of the Mn–Au edges of the Mn₂Au triangle, so that it occupies an equatorial position in the coordination sphere around manganese.

As stated above, reaction of compounds **10** with tedip give first a blue intermediate which could not be isolated. Its IR and low-temperature ³¹P NMR spectra, however, are similar to those of compounds **11**; therefore, we trust that this intermediate is just an unstable isomer of the final clusters isolated. This unstable intermediate then evolves in two different ways, one leading to the tetranuclear clusters **11** and a second one leading to the trinuclear clusters **12**. The latter reaction can be represented through eq 1.



The formation of **12** would perhaps be initiated by an intramolecular P–O bond oxidative addition of tedip to yield bridging phosphide (P(OEt)₂) and phosphonate

Chart 7



(OP(OEt)₂) groups, followed by extrusion of a gold phosphonate moiety and capture of some CO present in the solution. A close precedent for this rare process can be found in the electron-precise manganese–gold clusters [Mn₂Au₂{ μ -P(OEt)₂}{ μ -OP(OEt)₂}(CO)₆(PR₃)₂], which experience loss of the phosphonate group under various conditions to give the unsaturated pentanuclear clusters [Mn₂Au₃{ μ -P(OEt)₂}(CO)₆(PR₃)₃].⁸

Electron-Donor Properties of the Unsaturated Clusters 10. Compound **10b** reacts instantaneously with HBF₄·OEt₂ in dichloromethane solution to give the blue cationic cluster [Mn₂Au₂(μ_3 -H)(CO)₆(μ -dppm){P(*p*-tol)₃}₂]BF₄ (**13**). Spectroscopic data for **13** are almost identical with those for [Mn₂Au₂(μ_3 -H)(CO)₆(μ -dppm)-(PPh₃)₂]PF₆, an unsaturated cluster prepared upon addition of [AuPPh₃]⁺ to the trinuclear hydride cluster [Mn₂Au(μ -H)(CO)₆(μ -dppm)(PPh₃)] and characterized through an X-ray study mentioned above.¹¹ This structure is derived from that of clusters **10** by formally adding a proton to one of the Mn₂Au faces, on the side closer to the bridging dppm (Chart 7). Of course, it is reasonable to assume that initial attack of H⁺ occurs first on the side opposite the dppm bridge, and then the hydride rearranges upward, which implies the bending of one of the Mn₂Au triangles away from dppm. This possibly removes some of the steric congestion imposed by a flat Mn₂Au₂ skeleton. In addition, we recall that this metal skeleton is fluxional, as previously found for the PPh₃ analogue of **13**,¹¹ thus indicating that both the H ligand and the Au–PR₃ groups have substantial mobility in these clusters.

The IR spectrum of **13** exhibits four CO stretching bands that are 48 cm^{−1} higher on average than those in the parent cluster **10b**. This is expected and is indicative of a substantial electron density flow away from the dimanganese center, thus justifying our view of this reaction as an acid (H⁺)–base (Mn₂Au center) interaction.

Reaction of Compound 10b with SnCl₂. Having examined the reactions of clusters **10** with simple bases (phosphines) and acids (HBF₄·OEt₂), we then considered the reactions with methylene and related metal fragments. Taking into account the general isolobal relationships,^{28,29} reaction of a doubly metal–metal bonded compound with such a fragment can be considered a cyclopropanation-like reaction, which makes use of both donor and acceptor properties of the multiple metal–metal bond.

(28) (a) Hoffmann, R. *Angew. Chem., Int. Ed. Engl.* **1982**, *21*, 711. (b) Stone, F. G. A. *Angew. Chem., Int. Ed. Engl.* **1984**, *23*, 89.

(29) Adams, R. D. In *Comprehensive Organometallic Chemistry*, 2nd ed.; Abel, E. W., Stone, F. G. A., Wilkinson, G., Eds.; Pergamon: Oxford, U.K., 1995; Vol. 10, Chapter 1.

(27) Lee, K. H.; Low, P. M. N.; Hor, T. S. A.; Wen, Y.-S.; Liu, L. K. *Organometallics* **2001**, *20*, 3250.

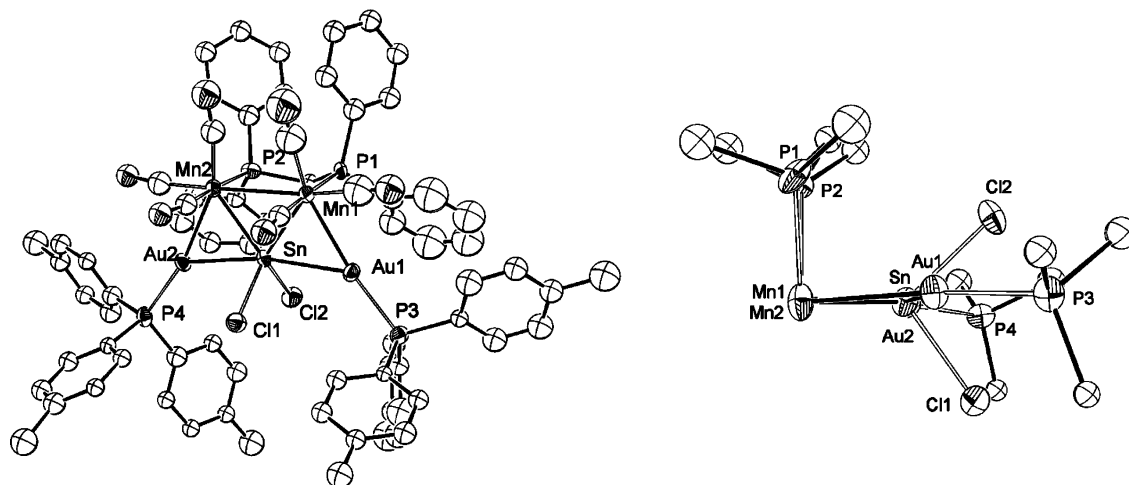


Figure 2. Molecular structure of compound **14** (left) and its projection along the Mn–Mn bond (right; CO ligands omitted and only C–P atoms of phosphine ligands shown for clarity). Ellipsoids represent 30% probability.

Diazomethane indeed reacts rapidly with **10b**, but this gives a mixture of complexes, which could not be separated or characterized. On the other extreme, no reaction was observed between **10b** and $[\text{Fe}_2(\text{CO})_9]$, the latter being a common source for the 16-electron fragment $\text{Fe}(\text{CO})_4$. This possibly has an steric origin, as the iron fragment might be too large for an already crowded dimanganese center. We then examined the reaction of **10b** with SnCl_2 , a much smaller metal analogue of methylene.

Compound **10b** reacts slowly with SnCl_2 in tetrahydrofuran to give the pentanuclear cluster $[\text{Mn}_2\text{Au}_2\text{SnCl}_2(\text{CO})_6(\mu\text{-dppm})\{\text{P}(p\text{-tol})_3\}_2]$ (**14**) in good yield. No intermediate species could be detected during this slow reaction. The IR spectrum of **14** (Table 1) exhibits five strong CO stretching bands with a frequency average similar to that of **10b**. This suggests that the incoming SnCl_2 fragment is not behaving as a pure donor or acceptor but possibly in both ways, as expected for a methylene-like metal fragment. However, the pattern of the CO bands in **14** is quite different from those for common $[\text{Mn}_2(\mu\text{-X})(\mu\text{-Y})(\text{CO})_6(\mu\text{-L}_2)]$ hexacarbonyl complexes, thus suggesting a considerable structural reorganization upon reaction, as confirmed through an X-ray study (Figure 2 and Table 2).

The structure of **14** exhibits a nearly planar raft-like pentanuclear $\text{Mn}_2\text{Au}_2\text{Sn}$ array with the tin atom as the common vertex of the three (Mn_2Sn or MnAuSn) metal triangles (maximum deviations from the mean plane are 0.101(7) Å for Mn(1) and 0.106(6) Å for Mn(2), on opposite sides). The diphosphine ligand bridges the Mn–Mn edge almost perpendicularly to this plane, and three carbonyls complete a distorted-octahedral environment around each Mn atom. The chloride ligands are bound to the tin atom and lie in a plane perpendicular to the $\text{Mn}_2\text{Au}_2\text{Sn}$ array. As for **10b**, consideration of 3c–2e bonds in the two MnSnAu triangles, with the corresponding orbitals pointing to the center of these triangles, leads to a regular description of the coordination geometry around the metal atoms, it being octahedral (Mn), tetrahedral (Sn), or linear (Au).

The Mn–Mn length (3.171(9) Å) is ca. 0.3 Å longer than that in **10b**, as expected upon changing the formal bond order from 2 to 1. This value is somewhat greater than those for the related electron-precise trinuclear

clusters $[\text{Mn}_2\text{Au}(\mu\text{-Br})(\text{CO})_6(\mu\text{-tedip})(\text{PPh}_3)]$ (3.090(3) Å)²⁴ and $[\text{Mn}_2\text{Au}(\mu\text{-PPh}_2)(\text{CO})_8(\text{PPh}_3)]$ (3.066(8) Å)³⁰ but similar to the Mn–Mn length in the also saturated $[\text{Mn}_2(\mu\text{-SnPh}_2)_2(\text{CO})_6(\mu\text{-tedip})]$ (3.1045(5) Å).³¹ The Mn–Au (2.651(7) and 2.654(6) Å) and Mn–Sn (2.602(7) and 2.600(7) Å) distances for **14** are similar to those in the aforementioned clusters. On the other hand, the Sn–Au lengths in **14**, 2.813(4) and 2.815(4) Å, are comparable to that of 2.881(1) Å found in $[(\text{PMe}_2\text{Ph})_2\text{AuSnCl}_3]$ ³² and are thus possibly indicative of a rather weak Sn–Au bonding interaction. Finally, we should note the presence of a weak interaction of the Au atoms with the carbonyls lying on the metal plane, as revealed by the relatively short Au–C separations of 2.53(4) and 2.63(6) Å (Table 2).

The metal skeleton in **14** is rather unusual. Heterometallic clusters with planar skeletons are rare, and most of the known examples involve transition metals and group 11 elements.^{7,9} In fact, to the best of our knowledge, compound **14** represents the first example of a pentanuclear raft-type heterometallic cluster having tin in the metal skeleton. The closest analogue of **14** would possibly be represented by the tetranuclear cluster $[\text{Os}_3(\mu\text{-SnCl}_2)(\mu\text{-CH}_2)(\text{CO})_{11}]$, a compound formed by insertion of SnCl_2 into one of the Os–Os bonds in $[\text{Os}_3(\mu\text{-CH}_2)(\mu\text{-CO})(\text{CO})_{10}]$.³³ Indeed, the formation of **14** can be understood as an insertion of SnCl_2 into an Mn–Au bond in **10b**, followed by rearrangement of the second AuPR_3 unit in order to bridge a Mn–Sn bond. Recalling the isolobal relationships in the pairs H/ AuPR_3 and $\text{CH}_2/\text{SnCl}_2$, the first step is completely analogous to the methylene insertion into the unsaturated $\text{Os}_2(\mu\text{-H})_2$ moiety of $[\text{Os}_3(\mu\text{-H})_2(\text{CO})_{10}]$ (Scheme 1).³⁴ The second step, which would lead to a coordinated methane molecule at the dimetal center, is not spontaneous in the triosmium system. We have previously shown, however, that these rearrangements conform to

(30) Iggo, J. A.; Mays, M. J.; Raithby, P. R.; Henrick, K. *J. Chem. Soc., Dalton Trans.* **1984**, 633.

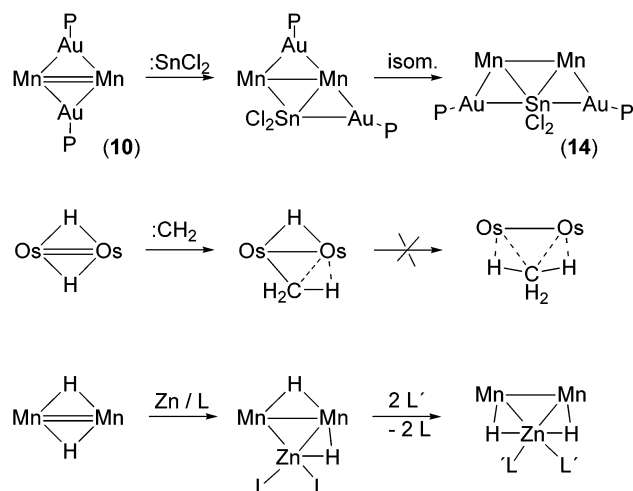
(31) Carreño, R.; Riera, V.; Ruiz, M. A.; Jeannin, Y.; Philoche-Levisalles, M. *J. Chem. Soc., Chem. Commun.* **1990**, 15.

(32) Clegg, W. *Acta Crystallogr.* **1978**, B34, 278.

(33) Viswanathan, N.; Morrison, E. D.; Geoffroy, G. L.; Geib, S. J.; Rheingold, A. L. *Inorg. Chem.* **1986**, 25, 3100.

(34) (a) Calvert, R. B.; Shapley, J. R. *J. Am. Chem. Soc.* **1977**, 99, 5225. (b) Calvert, R. B.; Shapley, J. R. *J. Am. Chem. Soc.* **1978**, 100, 7726.

Scheme 1. Formation of Cluster 14 in Comparison with Other Insertion Reactions of Unsaturated Dimetal Centers^a



^a Only the reactive centers are shown for clarity (see text).

a rather subtle balance of factors. Thus, the zinc derivatives of $[\text{Mn}_2(\mu\text{-H})_2(\text{CO})_6(\mu\text{-tedip})]$ adopt a methylene-like geometry for L = tetrahydrofuran but a methane-like arrangement for L' = $\text{Me}_2\text{N}(\text{CH}_2)_2\text{NMe}_2$ (Scheme 1).^{10a}

Concluding Remarks. Anions **1** and **2** are valuable, and in some cases unique, synthetic precursors for electron-deficient manganese–silver and –gold clusters having Mn_2M or Mn_2M_2 skeletons. These are formally derived through replacement of bridging H by MPR_3 units in the parent unsaturated dihydride $[\text{Mn}_2(\mu\text{-H})_2(\text{CO})_6(\mu\text{-dppm})]$. This substitution increases considerably the electron-donor ability of the dimanganese center while retaining some of the reactivity derived from its electron deficiency, best shown through the reaction with the carbene-like fragment SnCl_2 . However, considerable crowding is apparent in these tetranuclear Mn_2M_2 clusters; therefore, their reaction with simple P-donor ligands results in substitution of peripheral ligands or more complex transformations, rather than leading to simple addition processes.

Experimental Section

General Considerations. All manipulations and reactions were carried out using standard Schlenk techniques under an atmosphere of dry, oxygen-free nitrogen. Solvents were purified according to standard literature procedures³⁵ and distilled under nitrogen prior to use. Petroleum ether refers to that fraction distilling in the range 60–65 °C. The compounds $[\text{Mn}_2(\mu\text{-H})_2(\text{CO})_6(\mu\text{-dppm})]$,^{13a} $[\text{Mn}_2(\text{CO})_8(\mu\text{-dppm})]$,¹⁹ $[\text{AgCl}(\text{PCy}_3)]_4$,³⁶ and $[\text{AuCl}(\text{PR}_3)]$ (R = Ph, *p*-tol)³⁷ were prepared according to literature procedures. Tetrahydrofuran solutions of $\text{Na}_2[\text{Mn}_2(\text{CO})_6(\mu\text{-dppm})]$ were prepared in situ as described in ref 2 and used assuming a 100% yield. Other reagents were obtained from the usual commercial suppliers and used without further purification. Filtrations were carried out using a cannula or, more generally, through diatomaceous earth, and aluminum oxide (alumina) for column chromatography was deactivated by appropriate addition of water to the commercial

material (Aldrich, neutral, activity I). Low-temperature chromatographic separations were carried out using jacketed columns refrigerated by a closed 2-propanol circuit kept at the desired temperature with a cryostat. NMR spectra were recorded at 300.13 MHz (^1H), 121.50 MHz ($^{31}\text{P}\{^1\text{H}\}$), and 75.47 MHz ($^{13}\text{C}\{^1\text{H}\}$), at room temperature unless otherwise stated. Chemical shifts (δ) are given in ppm, relative to internal TMS (^1H , ^{13}C) or external 85% H_3PO_4 aqueous solution (^{31}P), with positive values for frequencies higher than that of the reference. Coupling constants (J) are given in Hertz. $^{13}\text{C}\{^1\text{H}\}$ NMR spectra were routinely recorded on solutions containing a small amount of tris(acetylacetonato)chromium(III) as a relaxation reagent. Occasionally, non-deuterated solvents were used, in which case a coaxial capillary containing D_2O was immersed into the solution, to adjust and maintain the homogeneity of the magnetic field. This is indicated as (solvent/ D_2O).

Preparation of Tetrahydrofuran Solutions of $\text{Li}[\text{Mn}_2(\mu\text{-H})_2(\text{CO})_6(\mu\text{-dppm})]$ (2**).** In a typical experiment, a THF solution (10 mL) of the dihydride $[\text{Mn}_2(\mu\text{-H})_2(\text{CO})_6(\mu\text{-dppm})]$ (0.033 g, 0.05 mmol) was treated with $\text{Li}[\text{BHET}_3]$ (50 μL of a 1 M solution in THF, 0.05 mmol), and the mixture was stirred for 30 min, yielding a dark brown solution which was then ready for further use. ^{31}P and ^1H NMR spectra indicate the presence of compound **2** as the major species in this air-sensitive solution. ^1H NMR (THF/ D_2O): δ –11.2 (t, br, J_{PH} = 28, $\mu\text{-H}$).

Preparation of Tetrahydrofuran Solutions of $\text{Na}[\text{Mn}_2(\mu\text{-H})_2(\text{CO})_6(\mu\text{-dppm})]$ (2**).** In a typical experiment, a THF solution (10 mL) of the dihydride $[\text{Mn}_2(\mu\text{-H})_2(\text{CO})_6(\mu\text{-dppm})]$ (0.035 g, 0.053 mmol) was stirred with an excess of $\text{Na}[\text{BH}_4]$ (ca. 0.02 g) for 30 min to give a yellow solution, which was filtered using a cannula and was then ready for further use. Alternatively, the solvent can be removed from the yellow solution, the residue extracted with dichloromethane, and the extract filtered through diatomaceous earth. Removal of solvent under vacuum from this filtrate gave a yellow powder that was washed with petroleum ether. This air-sensitive solid was shown by ^1H NMR to retain a considerable amount of THF. ^1H NMR (CD_2Cl_2): δ 7.50–6.50 (m, 20H, Ph), 3.54 (t, J_{PH} = 14, 2H, CH_2), –13.98 (s, br, 3H, Mn–H).

Preparation of Tetrahydrofuran Solutions of $\text{Na}_2[\text{Mn}_2(\text{CO})_8(\mu\text{-dppm})]$ (4**).** In a typical experiment, a THF solution (10 mL) of $[\text{Mn}_2(\text{CO})_8(\mu\text{-dppm})]$ (0.072 g, 0.1 mmol) was stirred at room temperature with an excess of a 0.6% Na amalgam (ca. 0.5 mL) to give an air-sensitive orange-brown solution, which was filtered using a cannula and was then ready for further use.

Preparation of $[\text{Mn}_2\text{H}_2(\text{CO})_8(\mu\text{-dppm})]$ (5**).** An excess of H_3PO_4 (0.05 mL of an aqueous 85% solution) was added to a THF solution of anion **4** prepared as described above from 0.1 mmol of starting material, and the mixture was stirred for 5 min to give a yellow solution. Solvent was then removed under vacuum, the residue was extracted with the minimum amount of dichloromethane, and the extract was chromatographed on alumina (activity III). Elution with dichloromethane/petroleum ether (1/6) gave a yellow fraction which yielded, after removal of solvents under vacuum, compound **5** as a yellow microcrystalline powder (0.059 g, 82%). Anal. Calcd for $\text{C}_{33}\text{H}_{24}\text{Mn}_2\text{O}_8\text{P}_2$: C, 55.02; H, 3.36. Found: C, 54.55; H, 3.10. ^1H NMR (C_6D_6): δ 7.43 (m, 8H, Ph), 6.85 (m, 12H, Ph), 3.84 (t, J_{PH} = 8, 2H, CH_2), –7.26 (false d, AA'XX' multiplet, $|J_{\text{PH}} + J_{\text{PH}}|$ = 40, 2H, Mn–H).

Preparation of $[\text{Mn}_2\text{Ag}(\mu\text{-H})(\text{CO})_6(\mu\text{-dppm})(\text{PCy}_3)]$ (6**).** Solid $[\text{AgCl}(\text{PCy}_3)]_4$ (0.021 g, 0.05 mequiv) was added to a THF solution containing ca. 0.05 mmol of compound **2**, prepared in situ as described above and cooled to 0 °C, and the mixture was stirred and allowed to reach room temperature over 20 min to yield a blue-violet solution. Solvent was then removed under vacuum, the residue was extracted with the minimum amount of dichloromethane, and the extract was chromatographed at –20 °C on an alumina column (activity IV). Elution

(35) Perrin, D. D.; Armarego, W. L. F. *Purification of Laboratory Chemicals*; Pergamon Press: Oxford, U.K., 1988.

(36) Cariati, F.; Naldini, L. *Gazz. Chim. Ital.* **1965**, 95, 201.

(37) Braunstein, P.; Lehner, H.; Matt, D. *Inorg. Synth.* **1990**, 27, 218.

with dichloromethane/petroleum ether (1/3) gave a blue fraction. Removal of solvents from that fraction yielded compound **6** as a blue-violet microcrystalline powder (0.030 g, 57%). Anal. Calcd for $C_{49}H_{56}AgMn_2O_6P_3$: C, 55.96; H, 5.37; Found: C, 56.30; H, 5.50. 1H NMR (CD_2Cl_2 , 233 K): δ 7.75–6.65 (m, 20H, Ph), 4.10, 3.83 (2 \times m, 2H, CH_2P), 1.80–0.90 (m, 33H, Cy), –20.6 (t, J_{PH} = 25, μ -H).

Preparation of $[Mn_2Au(\mu-H)(CO)_6(\mu-dppm)\{P(p-tol)_3\}]$ (7). The procedure is completely analogous to that described for **6**, except that $[AuCl\{P(p-tol)_3\}]$ (0.027 g, 0.05 mmol) was used instead. After chromatographic purification, compound **7** was obtained as a blue-violet microcrystalline powder (0.032 g, 55%). Anal. Calcd for $C_{52}H_{44}AuMn_2O_6P_3$: C, 53.63; H, 3.81; Found: C, 53.49; H, 4.00. 1H NMR (CD_2Cl_2): δ 7.65–6.70 (m, 32H, Ph and *p*-tol), 3.68, 3.36 (2 \times c, J_{PH} = J_{HH} = 10, 2 \times 1H, CH_2), 1.97 (s, 9H, Me), –20.74 (t, J_{PH} = 24, 1H, μ -H).

Preparation of $[Mn_2Au(\mu-H)(CO)_7(\mu-dppm)\{P(p-tol)_3\}]$ (8). Carbon monoxide was gently bubbled through a THF solution (10 mL) of compound **7** (0.030 g, 0.025 mmol) at room temperature for 30 s, and the mixture was further stirred for 10 min to give a brown solution. Solvent was then removed under vacuum and the residue dissolved in toluene and crystallized from toluene/petroleum ether at –20 °C to give compound **7** as a brown microcrystalline powder (0.020 g, 60%). Anal. Calcd for $C_{53}H_{44}AuMn_2O_7P_3$: C, 53.37; H, 3.72; Found: C, 53.91; H, 3.38. 1H NMR (CD_2Cl_2): δ 7.62–7.05 (m, 32H, Ph and *p*-tol), 3.87 (t, J_{PH} = 10, 2H, CH_2), 2.43 (s, 9H, Me), –5.43 (dt, J_{PH} = 92, 18, 1H, μ -H). $^{13}C\{^1H\}$ NMR (CD_2Cl_2 , 213 K): δ 231.0 (s, br, 1 \times CO), 229.5 (m, br, 2 \times CO), 227.0 (m, br, 4 \times CO), 142.7 ($C^4(p-tol)$), 138.0, 137.0 (2 \times false t, $|J_{CP} + J_{CP}|$ = 40, 2 \times $C^1(Ph)$), 134.3–128.4 (*p*-tol and Ph), 126.4 (d, J_{CP} = 57, $C^1(p-tol)$), 50.2 (t, J_{CP} = 20, CH_2), 22.0 (s, Me).

Preparation of $[Mn_2Ag_2(CO)_6(\mu-dppm)(PCy_3)_2]$ (9). Solid $[AgCl(PCy_3)]_4$ (0.045 g, 0.106 mmol) was added to a tetrahydrofuran solution (10 mL) containing ca. 0.053 mmol of **1** at –80 °C, and the mixture was stirred and allowed to reach room temperature for 20 min. Solvent was then removed under vacuum from the dark blue solution, and the residue was dissolved in a minimum amount of dichloromethane and chromatographed on an alumina column (activity III) at –20 °C. A blue fraction was collected by elution with dichloromethane/petroleum ether (1/5). Removal of solvents from the latter under vacuum gave compound **9** as a blue-violet microcrystalline powder (0.052 g, 68%). Anal. Calcd for $C_{67}H_{88}Ag_2Mn_2O_6P_4$: C, 55.93; H, 6.16; Found: C, 55.52; H, 5.93. 1H NMR (CD_2Cl_2 , 218 K): δ 7.70–7.10 (m, 20H, Ph), 5.24 (t, J_{HP} = 10, 2H, CH_2), 1.90–1.15 (m, 66H, Cy).

Preparation of $[Mn_2Au_2(CO)_6(\mu-dppm)(PPh_3)_2]$ (10a). The procedure is completely analogous to that described for **9**, except that $[AuCl(PPh_3)]$ (0.052 g, 0.11 mmol) was used instead. After chromatographic purification (elution with dichloromethane/petroleum ether (1/3)) compound **10a** was obtained as a blue microcrystalline powder (0.058 g, 70%). Anal. Calcd for $C_{67}H_{52}Au_2Mn_2O_6P_4$: C, 50.90; H, 3.32; Found: C, 51.42; H, 3.62. 1H NMR (CD_2Cl_2): δ 7.70–6.90 (m, 50H, Ph), 4.87 (t, J_{HP} = 9, 2H, CH_2).

Preparation of $[Mn_2Au_2(CO)_6(\mu-dppm)\{P(p-tol)_3\}_2]$ (10b). The procedure is completely analogous to that described for **10a**, except that $[AuCl\{P(p-tol)_3\}]$ (0.060 g, 0.11 mmol) was used instead. In this way compound **10b** was obtained as a dark blue microcrystalline solid (0.064 g, 72%). Anal. Calcd for $C_{73}H_{64}Au_2Mn_2O_6P_4$: C, 52.66; H, 3.87; Found: C, 52.17; H, 3.87. The crystals used in the X-ray study were grown by slow diffusion of petroleum ether into a toluene solution of the complex, at room temperature. 1H NMR (CD_2Cl_2): δ 7.70–6.90 (m, 44H, Ph and *p*-tol), 4.88 (t, J_{HP} = 10, 2H, CH_2), 2.40 (s, 18H, Me).

Reaction of Compound 10a with tedip. A tetrahydrofuran solution of compound **10a** (0.065 g, 0.041 mmol) was stirred with tedip (10 μ L, 0.041 mmol) at 0 °C for 5 min to give a black-blue solution, which was further stirred at room

temperature for 1 h. Solvent was then removed under vacuum, the residue was extracted with the minimum amount of dichloromethane, and the extract was chromatographed on an alumina column (activity III) at –30 °C. Elution with dichloromethane/petroleum ether (1/3) gave an orange fraction, which after removal of solvents yielded compound **12a** (0.012 g, 24%) as an orange microcrystalline powder. Elution with a 3/1 solvent mixture gave a blue-violet fraction which gave analogously compound **11a** as a blue-violet microcrystalline powder (0.037 g, 62%). Anal. Calcd for $C_{56}H_{57}Au_2Mn_2O_{10}P_5$ (**11a**): C, 43.43; H, 3.71; Found: C, 42.95; H, 3.42. Anal. Calcd for $C_{53}H_{47}AuMn_2O_8P_4$ (**12a**): C, 51.21; H, 3.81; Found: C, 50.75; H, 3.48. 1H NMR (**11a**, CD_2Cl_2): δ 7.60–6.80 (m, 35H, Ph), 4.30–3.50 (m, 10H, CH_2 and OCH_2), 1.39, 1.35, 1.34, 1.22, 1.16, 1.06 (complex, 6 \times t, 12H, Me); this corresponds to a mixture of isomers **A** and **B** in a 1:2 ratio (by ^{31}P NMR, see discussion and Table 3). 1H NMR (**12a**, CD_2Cl_2): δ 7.80–6.55 (m, 35H, Ph), 4.22 (q, J_{HH} = J_{HP} = 7, 2H, OCH_2), 4.02 (cd, J_{HH} = 7, J_{HP} = 6, 2H, OCH_2), 3.53 (dt, J_{HH} = 12, J_{HP} = 10, 1H, CH_2), 2.41 (cd, J_{HH} = J_{HP} = 12, J_{HP} = 6, 1H, CH_2), 1.46, 1.36 (2 \times t, J_{HH} = 7, 2 \times 3H, Me).

Reaction of Compound 10b with tedip. The procedure is completely parallel to that described above, but with compound **10b** (0.060 g, 0.036 mmol) used instead. After a similar workup, compounds **11b** (0.035 g, 72%) and **12b** (0.009 g, 20%) were obtained as blue-violet and orange microcrystalline powders, respectively. Anal. Calcd for $C_{59}H_{63}Au_2Mn_2O_{10}P_5$ (**11b**): C, 44.54; H, 3.99; Found: C, 45.00; H, 4.12. Anal. Calcd for $C_{56}H_{53}AuMn_2O_8P_4$ (**12b**): C, 52.35; H, 4.16; Found: C, 52.01; H, 3.85. 1H NMR (**11b**, 400.13 MHz, CD_2Cl_2): δ 7.55–6.65 (m, 32H, Ph and *p*-tol), 4.20–3.40 (m, 10H, CH_2 and OCH_2), 2.20 (s, C_6H_4Me , isomer **A**), 2.18 (s, C_6H_4Me , isomer **B**), 1.28, 1.07, 1.00 (3 \times t, 2:1:1 relative intensity, J_{HH} = 7, OCH_2CH_3 , isomer **B**), 1.282, 1.27, 1.14 (3 \times t, 2:1:1 rel int, J_{HH} = 7, OCH_2CH_3 , isomer **A**). Ratio **A**:**B** = 2:3. 1H NMR (**12b**, CD_2Cl_2): δ 7.60–6.50 (m, 32H, Ph and *p*-tol), 4.21 (q, J_{HH} = J_{HP} = 7, 2H, OCH_2), 4.02 (cd, J_{HH} = 7, J_{HP} = 6, 2H, OCH_2), 3.54 (dt, J_{HH} = 12, J_{HP} = 10, 1H, CH_2), 2.44 (s, 9H, C_6H_4Me), 2.37 (m, 1H, CH_2), 1.46, 1.35 (2 \times t, J_{HH} = 7, 2 \times 3H, OCH_2CH_3).

Preparation of $[Mn_2Au_2(\mu-H)(CO)_6(\mu-dppm)\{P(p-tol)_3\}_2]BF_4$ (13). A dichloromethane solution (10 mL) of compound **10b** (0.045 g, 0.027 mmol) was treated with $HBF_4 \cdot OEt_2$ (8 μ L of an 85% solution in Et_2O , ca. 0.04 mmol), and the mixture was stirred for 5 min. Solvent was then removed under vacuum and the residue washed with toluene (3 \times 3 mL) to give compound **13** as a dark blue microcrystalline solid (30 mg, 63%). Anal. Calcd for $C_{73}H_{65}Au_2BF_4Mn_2O_6P_4$: C, 50.02; H, 3.74; Found: C, 49.65; H, 3.52. 1H NMR (CD_2Cl_2): δ 7.57–7.08 (m, 44H, Ph and *p*-tol), 4.06 (t, J_{HP} = 12, 2H, CH_2), 2.15 (s, 18H, Me), –18.05 (tt, J_{HP} = 33, 22, 1H, μ -H).

Preparation of $[Mn_2Au_2SnCl_2(CO)_6(\mu-dppm)\{P(p-tol)_3\}_2]$ (14). Solid $SnCl_2$ (0.006 g, 0.032 mmol) was added to a tetrahydrofuran solution (10 mL) of compound **10b** (0.045 g, 0.027 mmol), and the mixture was stirred at room temperature for 12 h to give an orange mixture. Solvent was then removed under vacuum, and the residue was chromatographed on an alumina column (activity IV) at –30 °C. An orange fraction was collected by eluting with dichloromethane/petroleum ether (1/1). Removal of solvents from the latter gave compound **14** as an orange microcrystalline powder (0.038 g, 76%). Anal. Calcd for $C_{73}H_{64}Au_2Cl_2Mn_2O_6P_4Sn$: C, 47.28; H, 3.48; Found: C, 47.30; H, 3.77. The crystals used in the X-ray study were grown by slow diffusion of petroleum ether into a tetrahydrofuran solution of the complex at room temperature. 1H NMR (CD_2Cl_2): δ 7.60–6.65 (m, 44H, Ph and *p*-tol), 3.86 (dt, J_{HH} = 14, J_{HP} = 9, 1H, CH_2), 3.47 (dt, J_{HH} = 14, J_{HP} = 12, 1H, CH_2), 2.41 (s, br, 18H, Me).

X-ray Structure Determination for Compounds 10b and 14·1/2THF. Crystals of compound **10b** and of the THF solvate of **14** were obtained by crystallization from toluene/

Table 4. Crystallographic Data for **10b** and **14**· $\frac{1}{2}$ THF

	10b	14 · $\frac{1}{2}$ THF
empirical formula	C ₇₃ H ₆₄ Au ₂ Mn ₂ O ₆ P ₄	C ₇₅ H ₆₈ Au ₂ Cl ₂ Mn ₂ O _{6.5} P ₄ Sn
fw	1664.94	1890.58
temp (K)	293(2)	293(2)
wavelength (Å)	0.71073	0.71073
cryst syst, space group	triclinic, $P\bar{1}$	triclinic, $P\bar{1}$
<i>a</i> (Å)	12.048(5)	10.839(8)
<i>b</i> (Å)	12.364(5)	16.735(9)
<i>c</i> (Å)	25.136(9)	23.697(11)
α (deg)	85.38(2)	102.75(2)
β (deg)	78.45(2)	97.19(2)
γ (deg)	67.29(2)	100.27(2)
<i>V</i> (Å ³)	3384(2)	4064(4)
<i>Z</i> , calcd density (Mg m ⁻³)	2, 1.634	2, 1.545
abs coeff (mm ⁻¹)	4.832	4.393
<i>F</i> (000)	1636	1844
cryst size (mm)	0.35 × 0.20 × 0.15	0.25 × 0.20 × 0.15
θ range for data collec (deg)	3.03–25.01	3.03–22.67
index ranges	–13 ≤ <i>h</i> ≤ 14, –14 ≤ <i>k</i> ≤ 14, 0 ≤ <i>l</i> ≤ 29	0 ≤ <i>h</i> ≤ 9, –15 ≤ <i>k</i> ≤ 17, –22 ≤ <i>l</i> ≤ 23
no. of rflns collected/unique	11 797/11 797	2234/2234
no. of data/restraints/params	11 797/0/335	2234/20/338
goodness of fit on <i>F</i> ²	1.274	1.052
final <i>R</i> indices (<i>I</i> > 2σ(<i>I</i>)) (<i>R</i> 1, <i>wR</i> 2) ^a	0.0587, 0.1599	0.0501, 0.1166
<i>R</i> indices (all data) (<i>R</i> 1, <i>wR</i> 2) ^a	0.2702, 0.2620	0.0501, 0.1166
largest diff peak and hole (e Å ⁻³)	5.559 and –2.339	0.916 and –1.998

^a GOF = $[\sum(w(F_o^2 - F_c^2)^2)/(n - p)]^{1/2}$. *R*1 = $\sum||F_o| - |F_c||/\sum|F_o|$. *wR*2 = $[\sum[w(F_o^2 - F_c^2)]/\sum[w(F_o^2)^2]]^{1/2}$. *w* = $1/[\sigma^2(F_o^2) + (aP)^2 + bP]$, where *P* = $[\max(F_o^2, 0) + 2F_c^2]/3$.

petroleum ether and tetrahydrofuran, respectively, and crystals of suitable size were mounted on a Philips PW 1100 diffractometer with graphite-monochromated Mo K α radiation (λ = 0.710 73 Å). The data were collected at 293 K for both compounds. Crystallographic and experimental details are summarized in Table 4. A semiempirical method of absorption correction was applied (maximum and minimum values for the transmission coefficient were 1.000 and 0.907 (**10b**) and 1.000 and 0.732 (**14**· $\frac{1}{2}$ THF)).³⁸ No decay for **10b** but a decay of 18% was observed during the data collection for **14**· $\frac{1}{2}$ THF. The structures were solved by direct methods (SIR97)³⁹ and refined by least squares against *F*_o² (**10b**) and *F*_o (**14**· $\frac{1}{2}$ THF) (SHELXL-97),⁴⁰ using the WinGX software package.⁴¹ All the

non-hydrogen atoms were refined anisotropically for **10b** whereas for **14**· $\frac{1}{2}$ THF only Au, Mn, Sn, P, and Cl atoms were refined in this way. In **14**· $\frac{1}{2}$ THF two molecules of tetrahydrofuran, with an occupancy factor of 0.25, were found; moreover, two phenyl rings of the dpmm ligand were found disordered in two positions with an occupancy factor of 0.5. All the hydrogen atoms were introduced from geometrical calculations and refined using a riding model.

Acknowledgment. We thank the Ministerio de Educación y Ciencia and the Ministerio de Asuntos Exteriores of Spain for a grant (to X.-Y.L.) and the MECED and MCYT of Spain (Projects PB96-0317 and BQU2000-0944) for financial support.

Supporting Information Available: Tables of fractional atomic coordinates, anisotropic thermal parameters, and bond lengths and angles for compounds **10b** and **14**. This material is available free of charge via the Internet at <http://pubs.acs.org>.

OM0304614

(38) (a) Walker, N.; Stuart, D. *Acta Crystallogr., Sect. A* **1983**, *39*, 158. (b) Ugozzoli, F. *Comput. Chem.* **1987**, *11*, 109.

(39) Altomare, A.; Burla, M. C.; Camalli, M.; Cascarano, G. L.; Giacovazzo, C.; Guagliardi, A.; Moliterni, A. G. G.; Polidori, G.; Spagna, R. *J. Appl. Crystallogr.* **1999**, *32*, 115.

(40) Sheldrick, G. M. SHELX97: Programs for Crystal Structure Analysis (release 97-2); University of Gottingen, Gottingen, Germany, 1997.

(41) Farrugia, L. J. *J. Appl. Crystallogr.* **1999**, *32*, 837.